buildings

MDPI

Article

Evaluation of Waste Tire Rubber as an Alternative Aggregate in Geopolymer Mortars

Mehrzad Mohabbi * and Emre Bulsu

Department of Civil Engineering, Faculty of Engineering, Bingöl University, 12000 Bingöl, Türkiye; emrebulsu@gmail.com

* Correspondence: mmohabbi@bingol.edu.tr

Abstract

This study evaluates the potential of using Granulated Waste Tire Rubber (GWTR) as an alternative raw material in geopolymer mortars an eco-friendly, low-carbon alternative to traditional cement-based systems. The research investigates the synergistic effect of industrial by-products, such as slag (from ferrochrome plants) and fly ash (from thermal power plants), combined with varying proportions of GWTR (1/4, 1/3, and 1/2 by volume). A total of 22 mixtures were prepared using diverse binder pastes, including pure cement, slag-based, and fly ash-based geopolymer systems, alongside their cement-substituted derivatives. The mechanical and physical performances were assessed through compressive strength, flexural strength, and Ultrasonic Pulse Velocity (UPV) tests at 3, 7, 28, and 180 days, complemented by SEM microstructural analyses. The findings indicate that while GWTR significantly reduces the mechanical properties of pure cement matrices, this negative impact is substantially mitigated in geopolymer mortars supplemented with 5–10% cement. Mixtures containing 1/4 GWTR with 90–95% slag or fly ash (M6, M7, M15, M16) yielded the most successful results in terms of both strength and sustainability, specifically, mixtures M7 and M16 because the hybrid binder synergy effectively compensated for the rubber-induced porosity, ensuring a denser matrix and structural-grade compressive strength alongside high sustainability. Significant decreases in performance were observed at higher GWTR ratios, particularly at the 1/2 level. Overall, the study demonstrates that integrating GWTR into optimized geopolymer systems offers a viable pathway for the valorization of environmental waste and minimizing the ecological footprint of the construction industry.

Keywords: geopolymer mortar; waste tire rubber particles; compressive strength; flexural strength; microstructural analysis

Check for updates

Academic Editor: Eugeniusz Koda

Received: 31 March 2026
Revised: 23 April 2026
Accepted: 23 April 2026
Published: 28 April 2026

Copyright: © 2026 by the authors. Licensee MDPI, Basel, Switzerland. This article is an open access article distributed under the terms and conditions of the Creative Commons Attribution (CC BY) license.

1. Introduction

Although Portland cement is a vital binder for construction composites, its production is highly energy-intensive [1,2], emitting nearly one ton of CO_2 per ton produced [3,4]. Furthermore, the process depletes limited natural resources and relies heavily on coal for high-temperature calcination [5]. These challenges have driven global research toward eco-friendly alternatives with lower carbon footprints that integrate various wastes while matching or exceeding conventional performance [6]. Currently, innovative green geopolymer technology offers a nine-fold reduction in CO_2 emissions and a six-fold decrease in energy consumption [3]. By preventing resource depletion and providing exceptional structural performance, geopolymers effectively mitigate the impacts of global warming [2,3,5–7].

From this perspective, geopolymer technology represents an emerging global trend aimed at eliminating the environmental damage caused by cement use in the construction industry [8,9]. Cement ranks as the second most significant resource in terms of energy consumption [9,10]. The substantial energy requirements of cement production, coupled with the intensive extraction of natural resources, have led to both resource depletion and environmental pollution. This alternative to cement serves as a strategic solution to mitigate greenhouse gas emissions. Consequently, replacing cement with geopolymers derived from industrial by-products has become a highly viable alternative [9].

The rapid accumulation of End-of-Life Tires (ELTs) remains a critical environmental challenge, driven by increasing industrial demand. Globally, over 1.5 billion tires reach the end of their service life annually, primarily within land transportation systems. Conventional disposal methods, such as landfilling or incineration, pose severe environmental threats. These improper practices lead to the release of toxic emissions and the contamination of groundwater through atmospheric cycles, creating significant ecological risks [11]. This challenge has encouraged researchers to seek sustainable alternatives by integrating waste tire materials into construction composites. In alignment with circular economy principles, utilizing cementitious matrices enables the long-term sequestration and encapsulation of these wastes [12–14].

The origins of geopolymer technology trace back to 1930s aluminosilicate chemistry, eventually leading to the development of alkali-activated materials and zeolites [14]. A major milestone occurred in the 1970s with the definition of kaolinite-based geopolymer chemistry, which introduced fire-resistant, stone-like mineral polymers. Following the patenting of the first geopolymer resin in 1975 and 'Early High Strength Mineral Polymer' in 1984, these materials have evolved into a fundamental component of modern sustainable infrastructure [14].

Pham et al. [15] evaluated the dynamic performance of geopolymer mortars with 0–30% crumb rubber replacement. Split Hopkinson Pressure Bar tests demonstrated that increasing rubber content enhances impact resistance, energy absorption, and strain-rate sensitivity. The study concluded by establishing empirical formulas to predict dynamic increase factors (DIF) based on rubber substitution levels [15].

The study by Luhar et al. [16] highlights that replacing fine aggregates with waste tire fibers in geopolymer mortar is not just a cost-effective move, but a truly sustainable and user-friendly breakthrough. By scientifically evaluating key performance metrics such as compressive, flexural, and tensile strength, alongside elastic modulus and abrasion resistance, the research proves that this eco-friendly alternative consistently outperforms traditional OPC-based rubber mortars across the board [16].

Kuang et al. [17] investigated a modified geopolymer mortar by replacing 5% of river sand with rubber particles across four different sizes. Their findings show that while adding rubber slightly reduces fluidity and overall strength as particle size increases, the material achieves impressive early-stage durability. Specifically, heat curing at 80 °C boosted 1-day compressive and flexural strengths to 51.3 MPa and 8.2 MPa, respectively. However, the study notes that prolonged exposure to high temperatures eventually leads to a decline in these mechanical properties, suggesting that curing time is a critical factor for performance [17].

Lazorenko et al. [18] tackled the common strength loss in rubber-based geopolymer composites by investigating various physical and chemical pre-treatments for crumb rubber. Their research found that a potassium permanganate ($KMnO_4$) solution was the most effective, as its oxidative reaction more than doubled the rubber's hydrophilicity. This change created a much stronger bond between the rubber filler and the geopolymer matrix, successfully boosting compressive strength from 12.8 MPa to 15.5 MPa. The study suggests

that further refining the binder and curing process could yield even better mechanical results for these sustainable materials [18].

Zhang et al. [19] explored the sustainable recycling of fly ash, slag, and waste rubber by developing a modified geopolymer mortar. Their research found that a 10% crumb rubber replacement serves as the optimal "sweet spot," slightly enhancing compressive and tensile strength while significantly improving freeze–thaw resistance. While higher rubber content (20%) or the addition of OPC tended to degrade performance, the 10% ratio successfully minimized cracking and leveraged rubber's energy-dissipation qualities to boost overall durability.

A recent study by VanDomelen et al. investigated the sustainable development of geopolymer-based controlled low-strength materials (CLSM) by achieving a 100% replacement of conventional cement and sand with industrial by-products. The researchers utilized off-specification fly ash (OSFA) and bottom ash (BA)—both classified as potential environmental hazards—to formulate eco-friendly binders through alkali activation with sodium hydroxide. Their experimental program compared traditional two-part systems with user-friendly one-part geopolymer mixtures, focusing on the critical balance between high flowability and excavatable compressive strength. The findings revealed that while OSFA incorporation increased water demand by 15%, the one-part mixtures offered superior excavatability due to a stabilized strength development profile. Ultimately, VanDomelen et al. demonstrated that this upcycling approach not only mitigates the environmental risks associated with coal combustion waste but also offers a transformative economic advantage, reducing total material costs by up to 94%.

Wongsa et al. [20] developed lightweight geopolymer mortars by fully replacing river sand with 100% recycled crumb rubber. While this complete replacement significantly lowered compressive strength, it achieved a 42% reduction in density and a 79% drop in thermal conductivity compared to traditional sand-based mortars. The results suggest that these eco-friendly, high insulation geopolymers are ideal for producing lightweight masonry blocks that outperform conventional bricks in thermal efficiency.

dos Reis Ferreira et al. [21] used Response Surface Methodology to optimize geopolymer mortars containing rubber waste. Their analysis identified that a 1% rubber replacement combined with a 6-day curing period yielded the best results, achieving a compressive strength of 17.75 MPa. With an experimental error rate under 10%, the study successfully established a reliable model for predicting the performance of these eco-friendly composites [21].

Mermerdaş et al. [22] explored using waste tire crumbs (10–40%) in geopolymer composites, specifically testing if increasing binder content could mitigate the resulting loss in strength and fluidity. While rubber replacement naturally lowered density and thermal conductivity, boosting the binder content up to 800 kg/m^3 helped recover performance. Their findings show that with a controlled mixed design, these waste tires can be effectively repurposed into durable, eco-friendly construction materials.

Mabrouk et al. [23] investigated the impact of curing temperatures (80 °C and 100 °C), waste tire rubber, and silica fume on lightweight geopolymer composites. In their study, rubber replaced pumice aggregate by up to 45%, while silica fume substituted 20% of the slag content. Their comprehensive analysis using SEM, XRD, and TGA revealed that while adding rubber and silica fume increased porosity and water absorption, it also led to a decline in mechanical strength, particularly at higher curing temperatures. Thermal tests showed that while rubber increased mass loss under extreme heat, the inclusion of silica fume altered the chemical composition to improve the material's overall thermal stability and mechanical performance in specific mixes.

Yadollahi et al. [24] systematically evaluated the compressive strength of ferrochrome slag-based geopolymers by optimizing three critical design parameters: Na_2O concen-

tration, silica modulus, and water-to-binder ratio. By testing nine distinct formulations, the study demonstrated that precise control of these variables can yield high-strength, structural-grade geopolymers. Ultimately, the research provides a quantitative foundation for transforming industrial waste into sustainable binders, proving that ferrochrome slag is a viable and eco-friendly alternative for high-performance construction materials.

Yadollahi [25] evaluated the effects of nano- and micro-silica (2–10% dosages) on ferrochrome slag-based geopolymers. The results identified 6% nano-silica as the optimal dosage, significantly boosting compressive strength, tensile strength, and the elastic modulus. SEM analysis confirmed that this improvement is driven by a denser, more homogenous microstructure and enhanced bonding, proving nano-silica's potential to refine and strengthen slag-based binder systems.

Yadollahi et al. [26] addressed the environmental challenge of non-recyclable mineral wool waste by repurposing glass wool and rock wool into geopolymer binders. Activated with Na_2SiO_3 and NaOH, the study tested silica modulus ratios of 2.0, 2.5, and 3.0, identifying 2.5 as the optimal modulus. Mechanical tests conducted across various curing temperatures revealed that glass wool-based geopolymers achieved a peak compressive strength of 59.2 MPa when cured at 75 °C. These findings demonstrate the high potential of powdered mineral wool as a sustainable raw material for high strength geopolymer production.

The primary objective of this research is to fill the existing gap in the literature regarding the optimization of hybrid binders (ferrochrome slag, fly ash, and minor cement) to mitigate mechanical degradation in mortars containing high amounts of waste tire rubber.

2. Materials and Methods

2.1. Materials

In this study, Ferrochrome Slag (FCS) from Elazıg facilities (Eti Ferrochrome Co., Elazığ, Turkey) and Class F Fly Ash (FA) from the İskenderun Sugozu (İskenderun, Turkey) power plant were utilized as primary binders. To optimize reactivity, the FCS was ground to match cement fineness, passing through a 45 µm sieve, while the FA was selected for its low lime content in accordance with ASTM C618 standards. Although both materials exhibit particle size distributions within the 1 µm to 45 µm range, granulometric analysis confirms that FCS possesses a coarser and broader distribution compared to the finer and more homogenous particle structure of the fly ash.

The chemical and physical properties of fly ash and slag are detailed in Table 1, while their respective granulometric distribution curves are illustrated in Figure 1.

Table 1. Chemical composition of Elazig ferrochrome slag and fly ash (%).

Chemical Composition	Ferrochrome Slag	Fly Ash
CaO	1.10	4.81
SiO_2	33.80	44.23
Al_2O_3	25.48	19.60
Fe_2O_3	0.61	7.79
MgO	35.88	2.00
SO_3	----	0.14
K_2O	----	1.70
Na_2O	----	1.17
Cr_2O_3	2.12	------
Others	1.01	18.56

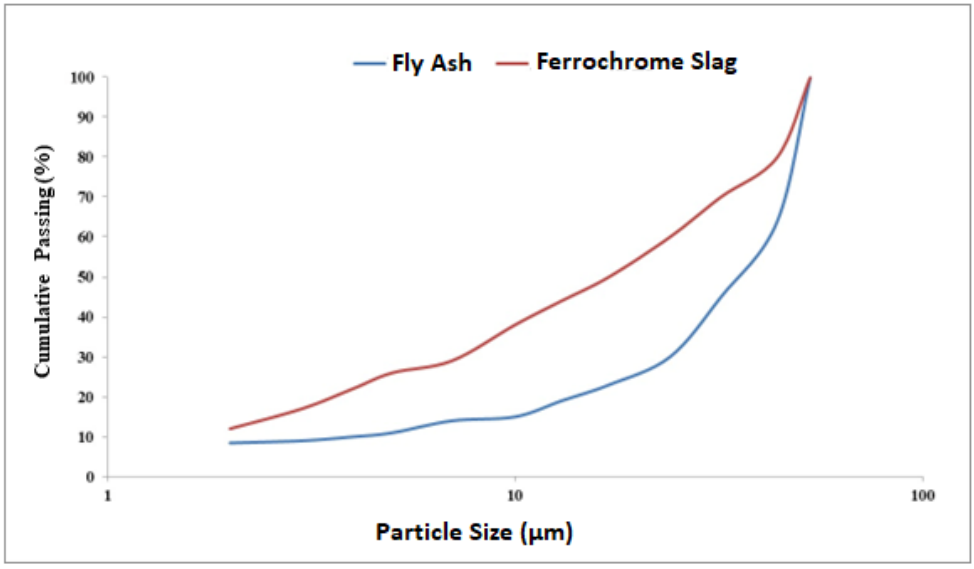


Figure 1. Particle size distribution (PSD) curves of fly ash and ferrochrome slag.

2.1.1. Alkali Activators

Sodium hydroxide (NaOH) and sodium silicate ($Na_2O\backslash SiO_2$) were employed as alkaline activators for the geopolymerization process. The NaOH, sourced from Merck with a purity of 99%, was utilized in a solution containing 32–33% sodium hydroxide and 67–68% water, providing a highly alkaline environment with a specific gravity of 1.35. Complementing this, sodium silicate commonly known as water glass was used in a colorless gel form, characterized by a chemical composition of 22–24% SiO_2, 11–12% Na_2O, and 64–67% H_2O. This silicate activator exhibited a specific gravity ranging between 1.380 and 1.397, serving as a critical catalyst to ensure a robust and stable geopolymer matrix.

2.1.2. Waste Tire Particles, Cement, and Mixing Water

Recycled waste tire particles, processed to pass through a 2 mm sieve, were utilized as the primary aggregate for the geopolymer mortar production. For the control mixtures, CEM-I 42.5 R type cement (Seza Cement Factory, Elazıg, Turkey) was employed as the binding agent. Additionally, potable tap water provided by Bingöl University was used as the mixing water for the cement-based mortars to ensure standardized quality across the samples.

2.2. Method

2.2.1. Mix Design and Specimen Preparation

In this study, a total of 22 distinct geopolymer formulations were developed across two primary groups. The first group utilized ground ferrochrome slag (FCS) as the main binder, while the second group incorporated fly ash (FA). The binder compositions were designed with 100%, 95%, and 90% FCS or FA by volume, with the remaining 5% and 10% substituted by CEM-I 42.5 R cement. Waste tire aggregates were integrated into these mixtures at volumetric ratios of 1/2, 1/3, and 1/4. Detailed mix proportions are summarized in Table 2.

The preparation process began with a 3 min pre-mixing of sodium hydroxide and sodium silicate solutions (maintaining a constant silica modulus of 3.0). Subsequently, the solid precursors and aggregates were added, and the mortar was mixed for one minute at low speed followed by one minute at high speed. The resulting fresh mortar was cast into 4 × 4 × 16 cm molds and compacted on a vibrating table for 60 s.

Table 2. Detailed mix proportions (gr).

Mix Code	GWTR	Ferrochrome Slag	Fly Ash	Cement	Na_2SiO_3	NaOH	Water
M1	0.0	0.0	0.0	600.0	0.0	0.0	270.0
M2	275.0	0.0	0.0	1420.0	0.0	0.0	416.7
M3	366.7	0.0	0.0	1255.1	0.0	0.0	370.3
M4	550.0	0.0	0.0	175.7	0.0	0.0	277.9
M5	275.0	1251.0	0.0	0.0	277.8	139.0	0.0
M6	275.0	1193.3	0.0	62.6	277.8	139.0	0.0
M7	275.0	1140.9	0.0	125.1	277.8	139.0	0.0
M8	366.7	1112.2	0.0	0.0	247.0	123.3	0.0
M9	366.7	1056.6	0.0	55.6	247.0	123.3	0.0
M10	366.7	1014.1	0.0	112.7	247.0	123.3	0.0
M11	550.0	834.1	0.0	0.0	185.2	92.6	0.0
M12	550.0	796.7	0.0	42.0	185.2	92.6	0.0
M13	550.0	760.6	0.0	84.5	185.2	92.6	0.0
M14	275.0	0.0	968.5	0.0	277.8	139.0	0.0
M15	275.0	0.0	923.9	48.4	277.8	139.0	0.0
M16	275.0	0.0	883.3	96.9	277.8	139.0	0.0
M17	366.7	0.0	861.0	0.0	247.0	123.3	0.0
M18	366.7	0.0	818.0	55.6	247.0	123.3	0.0
M19	366.7	0.0	785.1	112.7	247.0	123.3	0.0
M20	550.0	0.0	645.8	0.0	185.2	92.6	0.0
M21	550.0	0.0	616.8	42.0	185.2	92.6	0.0
M22	550.0	0.0	588.9	84.5	185.2	92.6	0.0

To accelerate geopolymerization and refine the microstructure, the specimens were wrapped in stretch film and subjected to heat curing at 75 °C for 24 h. This temperature was selected based on established literature indicating that curing within the 60–90 °C range significantly enhances mechanical performance compared to ambient conditions [27–34]. Following the thermal treatment, the specimens were stored under laboratory conditions until the scheduled testing dates.

The schematic representation of the geopolymerization process for fly ash and ferrochrome slag utilized in our study is illustrated step-by-step in the figure below: mechanical testing (Figure 2).

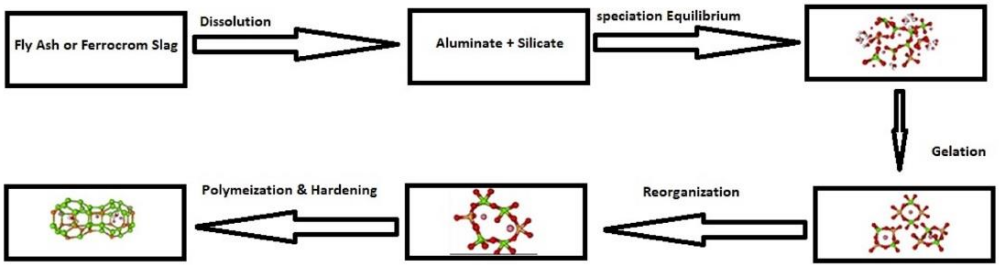


Figure 2. Schematic representation of the geopolymerization process for fly ash and ferrochrome slag.

In the fresh state analysis, the geopolymer mortars exhibited a rapid setting behavior (flash set), losing their plasticity within approximately 2.5 min as measured by the Vicat apparatus. This accelerated geopolymerization process, combined with the hydrophobic nature of GWTR particles, significantly limited the mobility of the mixtures, making standard slump-flow measurements impractical.

The mechanical performance of the geopolymer mortars was evaluated using 4 × 4 × 16 cm prismatic specimens, with three samples tested per mix. Flexural strength tests were conducted in accordance with ASTM C348 [35]. Following the flexural tests, the broken prism halves were repurposed to determine the compressive strength, resulting

in six 4 × 4 × 4 cm equivalent cube samples for each series. These compressive strength measurements were performed following the procedures outlined in ASTM C349 [36].

2.2.2. Microstructural Characterization

The microstructural and chemical evolution of the geopolymer specimens was characterized via Scanning Electron Microscopy (SEM). This analytical technique was employed to investigate the morphological features, interfacial transition zones (ITZ), and pore size distribution within the binder matrix, providing critical insights into the connectivity and homogeneity of the synthesized structures.

3. Experimental Results and Discussion

3.1. Compressive Strength Results

The compressive strength of the specimens, subjected to a 24 h heat curing at 75 °C, was evaluated at testing ages of 3, 7, 28, and 180 days. Following the flexural tests conducted on three 4 × 4 × 16 cm prisms per series, the resulting fragments were tested as 4 × 4 × 4 cm equivalent cubes, providing six samples for compressive strength measurement as shown in Figure 3. The final strength values for each mixture were determined by averaging the results of these six representative specimens.



Figure 3. Geopolymer mortar specimens containing waste tire aggregates subjected to compressive and flexural strength testing.

3.2. Evaluation of Slag-Based Geopolymers

Due to the extensive number of formulations, the results are categorized into two sections: slag-based (Figure 4) and fly ash-based (Figure 5) geopolymer mixtures. As illustrated in Figure 4, the reference mixture M1 (100% cement paste) exhibited the highest compressive strength across all testing ages, reaching 28.7 MPa at 3 days and 50.06 MPa at 180 days.

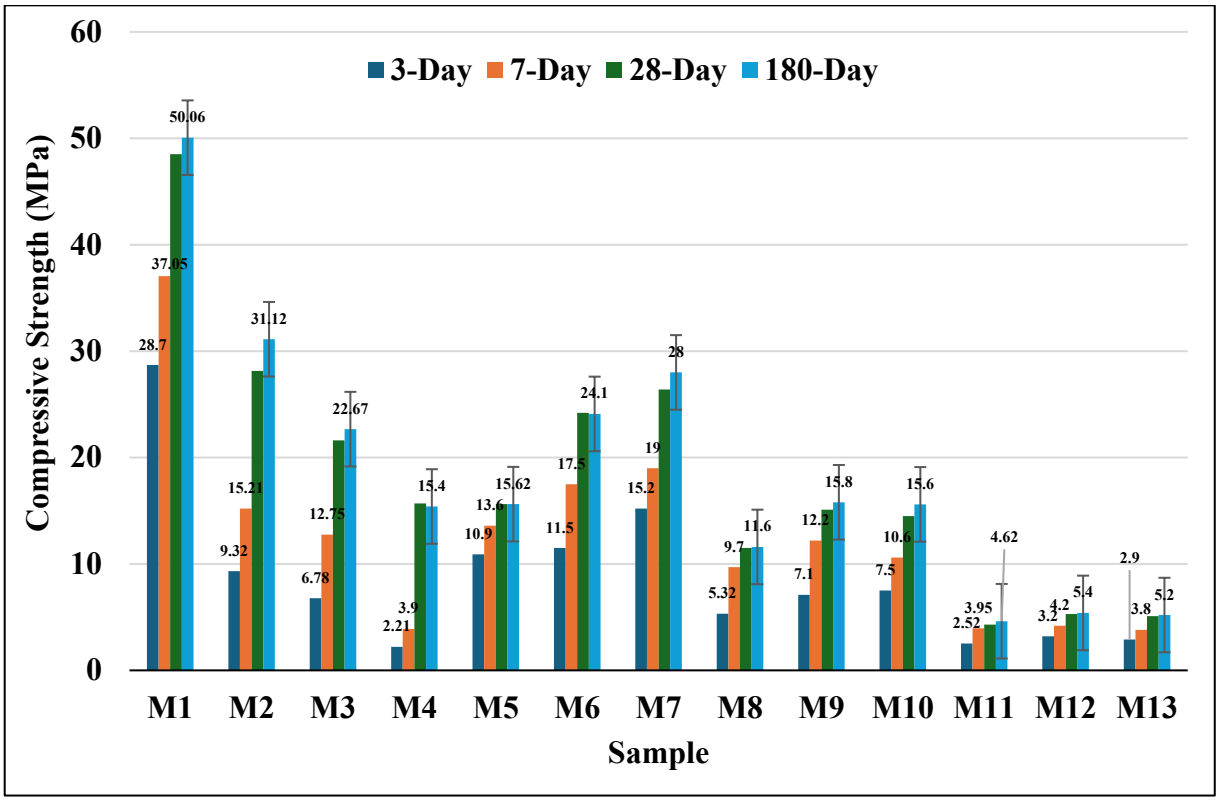


Figure 4. Compressive strength test results of geopolymer mortar specimens produced with ferrochrome slag.

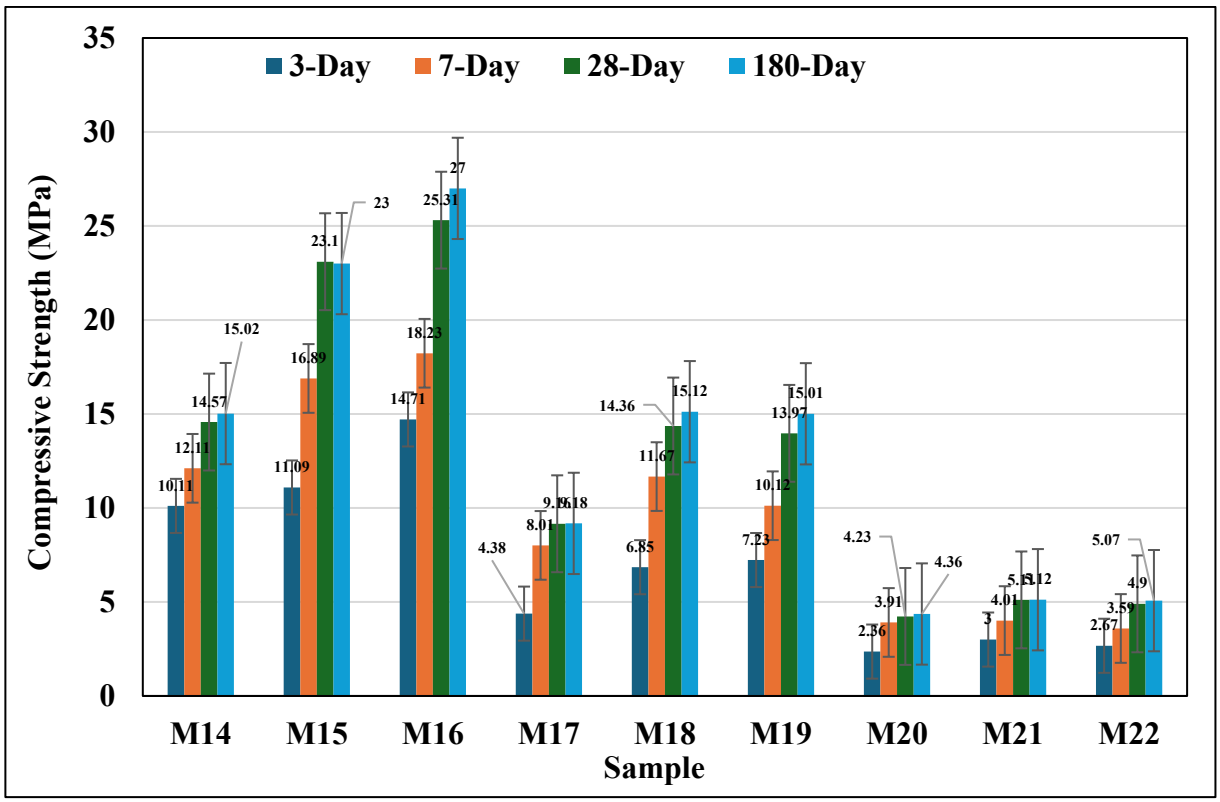


Figure 5. Compressive strength test results of geopolymer mortar specimens produced with fly ash.

In the control groups containing only cement and GWTR, a clear inverse correlation was observed: as the GWTR content increased, the compressive strength significantly

decreased. This trend is particularly evident in mixtures M2–M4, where the 180-day strengths were recorded as 31.12 MPa (M2—1/4 GWTR), 22.67 MPa (M3—1/3 GWTR), and 15.4 MPa (M4—1/2 GWTR).

While the incorporation of slag generally led to a reduction in strength compared to the pure cement reference, certain slag-based combinations demonstrated acceptable performance levels. Notably, mixture M7 performed remarkably well, achieving 26.4 MPa at 28 days and 28 MPa at 180 days. Similarly, the M6 mixture showed stable results with 24.2 MPa at 28 days and 24.1 MPa at 180 days. However, the simultaneous increase in slag and GWTR content accelerated the strength loss. For instance, mixtures with high GWTR content (1/2 by volume), such as M11–M13, exhibited low 180-day compressive strengths hovering around 4–5 MPa (Figure 4).

3.3. Early-Age Compressive Strength Analysis (3-Day)

In terms of 3-day compressive strength, the M1 mixture (100% cement paste) exhibited the highest performance at 28.7 MPa (Figure 4). This result is attributed to the rapid setting and hydration characteristic of cement, which typically provides high early-age strength. Notably, the M7 mixture achieved the second-highest strength at 15.2 MPa, suggesting that despite the low cement content, the incorporation of activators facilitated a robust early-stage reaction.

Furthermore, mixtures M6 (95% slag + 5% cement + 1/4 GWTR) and M5 (100% slag + 1/4 GWTR) both exceeded 10 MPa at 3 days, indicating that the slag contributes effectively to the strength development when properly activated. In contrast, mixtures with a 1/2 GWTR ratio (M4, M11, M12, and M13) consistently yielded low early-age performance, with values ranging between 2–3 MPa. These findings confirm that a higher GWTR content leads to a significant reduction in early-age strength development (Figure 4).

3.4. 7-Day Compressive Strength Analysis

At the 7-day testing stage, the M1 mixture maintained its superior performance with a peak compressive strength of 37.05 MPa (Figure 4), indicating the continued dominance of the cement hydration process. For the M7 and M6 mixtures, despite their significantly low cement content, the achieved strength values ranging between 17 and 19 MPa suggest that the contribution of the slag to the structural matrix becomes more pronounced after the first week of curing.

In contrast, the M3 mixture, composed solely of cement and GWTR, yielded a strength of 12.75 MPa, further demonstrating the diminishing effectiveness of the cement binder as the GWTR content increases. Mixtures within the M11–M13 range, characterized by a 1/2 GWTR ratio, continued to exhibit substantially low compressive strength values (Figure 4).

3.5. 28-Day Compressive Strength Analysis

At the 28-day curing stage, the M1 mixture reached a compressive strength of 48.51 MPa. Interestingly, the M2 and M7 mixtures yielded comparable results, with strengths recorded at 24 MPa and 26.4 MPa, respectively (Figure 4). It is noteworthy that despite the significantly lower cement content in M7, it achieved a strength level similar to that of M2. For mixtures such as M4, M5, M9, and M10, the compressive strength values hovered around the 14–16 MPa range. In contrast, mixtures incorporating a 1/2 GWTR ratio (M11–M13) exhibited very low compressive strengths, ranging between 4 and 5 MPa. These values indicate that such high-rubber content mixtures are structurally inadequate for load-bearing applications (Figure 4).

3.6. Long-Term (180-Day) Compressive Strength Analysis

Upon evaluating the 180-day compressive strength results (Figure 4), the M1 mixture reached a peak value of 50.06 MPa. Notably, both M2 and M7 mixtures achieved a strength

level of approximately 30 MPa. The fact that M7 attained such a high strength with only 10% cement content can be attributed to the prolonged hydration and latent hydraulic activity of the slag, which significantly enhances the long-term structural integrity of the matrix (Figure 4).

3.7. Comparative Evaluation and Sustainability Outlook

While the M1 mixture exhibited the highest overall compressive strength, M7 (1/4 GWTR + 90% slag + 10% cement) stands out as a highly favorable alternative, offering substantial long-term strength despite its low cement content, alongside significant ecological and economic benefits. Similarly, the M6 mixture (1/4 GWTR + 95% slag + 5% cement) provided structurally acceptable strength while further reducing the cement ratio. On the other hand, the M2 mixture (1/4 GWTR + 100% cement) maintained high strength performance notwithstanding the incorporation of GWTR (Figure 4).

Evaluating the overall results presented in Figure 5, it is observed that while the incorporation of fly ash tends to reduce strength, the addition of low GWTR and cement leads to a notable improvement in mechanical performance. For instance, the 180-day compressive strength was recorded as 15.02 MPa for the M14 mixture (25% GWTR, 100% fly ash). This value increased to 23 MPa for M15 (25% GWTR, 95% fly ash, 5% cement) and reached 27 MPa for M16 (25% GWTR, 90% fly ash, 10% cement). However, when the GWTR content was increased to 50%, a significant degradation in compressive strength was observed, regardless of the fly ash proportion (Figure 5).

Regarding the 3-day early-age results, it is evident that fly ash-based mixtures (M14–M16) contribute significantly to early strength development, even with low cement content (Figure 5). Conversely, mixtures containing 50% GWTR (M4 and M20–M22) exhibited remarkably low compressive strength. Due to this performance deficit, these specific blends are considered unsuitable for structural applications during the early curing stages (Figure 5).

The 7-day compressive strength tests reveal that fly ash and cement blends containing 25% GWTR, such as M15 and M16, exhibit strong potential for developing high strength in the mid-term. On the other hand, mixtures with a higher GWTR content of 33% (M17–M19) demonstrate a noticeably slower rate of strength development (Figure 5).

When evaluating the 28-day samples, the M16 mixture (90% fly ash, 10% cement, and 25% GWTR) exhibits compressive strength characteristics comparable to those of M2 (Figure 5). From a sustainability perspective, this performance suggests that M16 serves as a viable alternative to more traditional blends. Regarding the 33% GWTR content series, specifically the fly ash-based mixtures M18 and M19, the compressive strength reaches approximately 14 MPa. In contrast, geopolymer formulations with a 50% GWTR content continue to show significantly poor mechanical performance, with strength values stagnating around 4–5 MPa even at this curing age (Figure 5).

The 180-day compressive strength values serve as a key indicator of the material's long-term performance. The M16 mixture reached a significant strength milestone of 27 MPa at 180 days; this robust development is attributed to the late pozzolanic reaction of the fly ash, which effectively enhances the matrix over time. For geopolymers with a 33% GWTR content, such as M18 and M19, the compressive strength stabilizes around 15 MPa (Figure 5). Conversely, mixtures containing 50% GWTR (M20–M22) remain structurally insufficient, with strength values failing to exceed 6 MPa, thereby limiting their potential for load-bearing applications (Figure 5).

3.8. Flexural Strength Test Results of Geopolymer Mortar Samples

The flexural strength development of geopolymer mortars was significantly influenced by the binder type and fly ash (FA) content. While various combinations of slag and FA

were evaluated, the reference cement mixture (M1) consistently yielded the highest flexural strength values across all testing ages.

The reference cement mixture (M1) exhibited flexural strengths of 2.83, 4.13, 7.19, and 7.23 MPa at 3, 7, 28, and 180 days, respectively (Figure 6). This superior performance is attributed to the high early-age reactivity of cement as a primary binder. Conversely, increasing the fly ash (FA) content led to a significant decline in flexural strength. For instance, at 180 days, the strength dropped from 7.23 MPa in M1 to 3.23 MPa in the M2 mixture (1/4 FA ratio) and further decreased to 1.32 MPa in the M4 mixture (1/2 FA ratio). These findings suggest that the incorporation of fly ash (FA) adversely affects the binding properties and microstructural continuity of the geopolymer matrix. While slag-only mixtures (e.g., M5, M8, M11) exhibited limited flexural strength development, even minor cement additions significantly enhanced performance. Notably, the M6 mixture (95% slag + 5% cement) demonstrated an optimal flexural strength of 3.35 MPa at 180 days. Furthermore, the M7 mixture (90% slag + 10% cement) yielded a flexural strength of 2.5 MPa, which is lower than that of M6 (Figure 4). This suggests that mechanical performance depends not only on cement content but also on the microstructural alterations arising from the slag-cement interaction. In mixtures with high fly ash (FA) content—specifically those with a 1/2 ratio and minimal or no cement flexural strengths remained significantly low. For instance, the 180-day strengths for M11, M12, and M13 were measured at 0.47, 0.46, and 0.42 MPa, respectively. These values indicate that such compositions possess inadequate mechanical performance for structural applications.

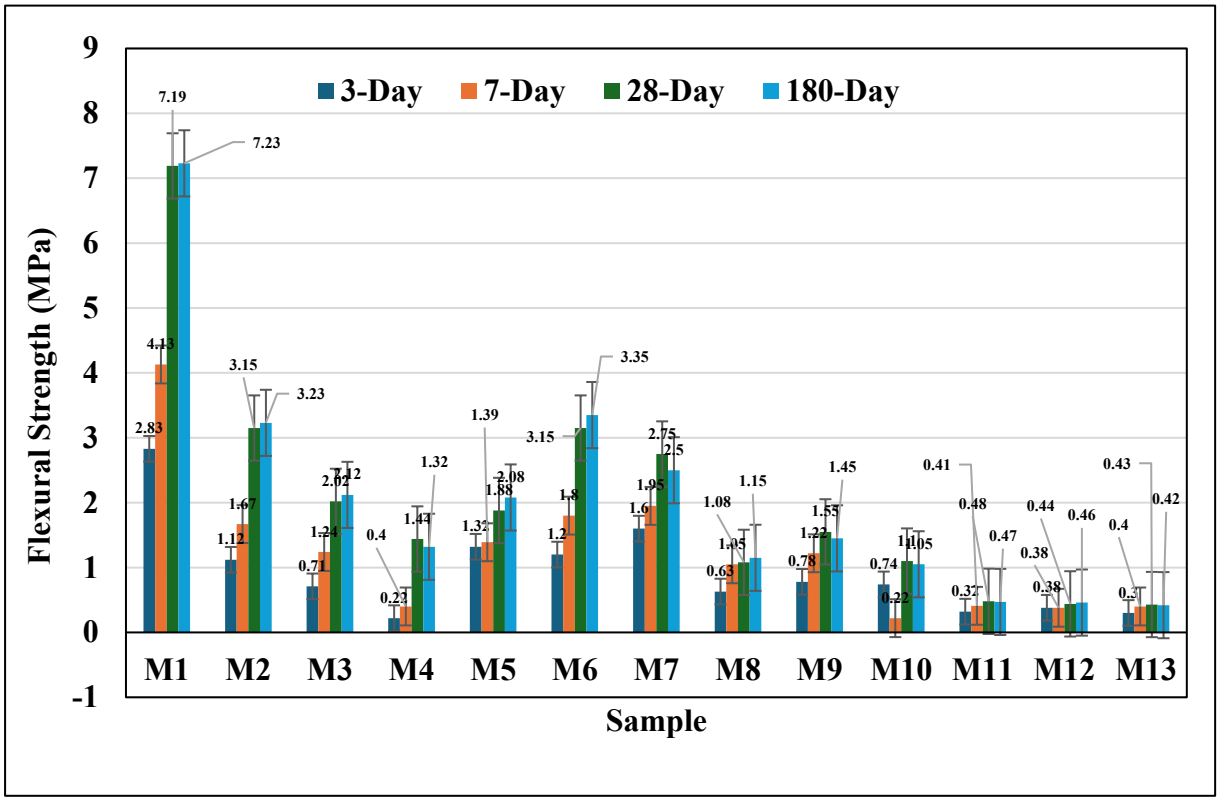


Figure 6. Flexural strength test results of geopolymer mortar specimens produced with ferrochrome slag.

The strength regression observed in M9 and M10 at 180 days is likely a consequence of long-term micro-crack propagation stemming from high alkali-induced chemical shrinkage, as evidenced by the SEM micrographs in Section 3.10.

The second group of mixtures focuses on fly ash (FA)-based geopolymers (Figure 7). The data clearly demonstrates that the FA ratio and binder composition are critical determinants of flexural strength. Increasing the FA content consistently led to performance degradation;

specifically, doubling the FA ratio from 25% (M2) to 50% (M4) caused the 28-day flexural strength to drop from 3.15 MPa to 1.44 MPa. This decline suggests that FA addition compromises the matrix continuity, thereby increasing strength loss. While geopolymers using only fly ash as a binder (e.g., M14) exhibited low strength values, the partial replacement of fly ash with cement significantly enhanced flexural performance. The inclusion of 5% cement in mixture M15 resulted in a 28-day flexural strength of 3.01 MPa, representing a nearly 75% increase compared to M14. This enhancement suggests that cement replacement improves the binding properties and reinforces the matrix bonds in fly ash-based geopolymers (Figure 7). Interestingly, increasing the cement content to 10% (e.g., M16 and M19) yielded similar or even lower strengths, indicating that 5% cement may be the optimum threshold for fly ash-cement interactions. Furthermore, higher cement ratios failed to provide the expected improvement in matrix integrity, particularly in mixtures with high fly ash (FA) content. Overall, the reference mixture (M1), composed of 100% cement, achieved the highest flexural strength across all testing ages, reaching 7.19 MPa at 28 days and 7.23 MPa at 180 days. These results underscore the critical role of the cement matrix in structural performance. Conversely, while the incorporation of fly ash (FA) in geopolymer mortar matrices offers significant environmental and economic advantages, it is observed to exert a distinct negative impact on mechanical performance (Figure 7).

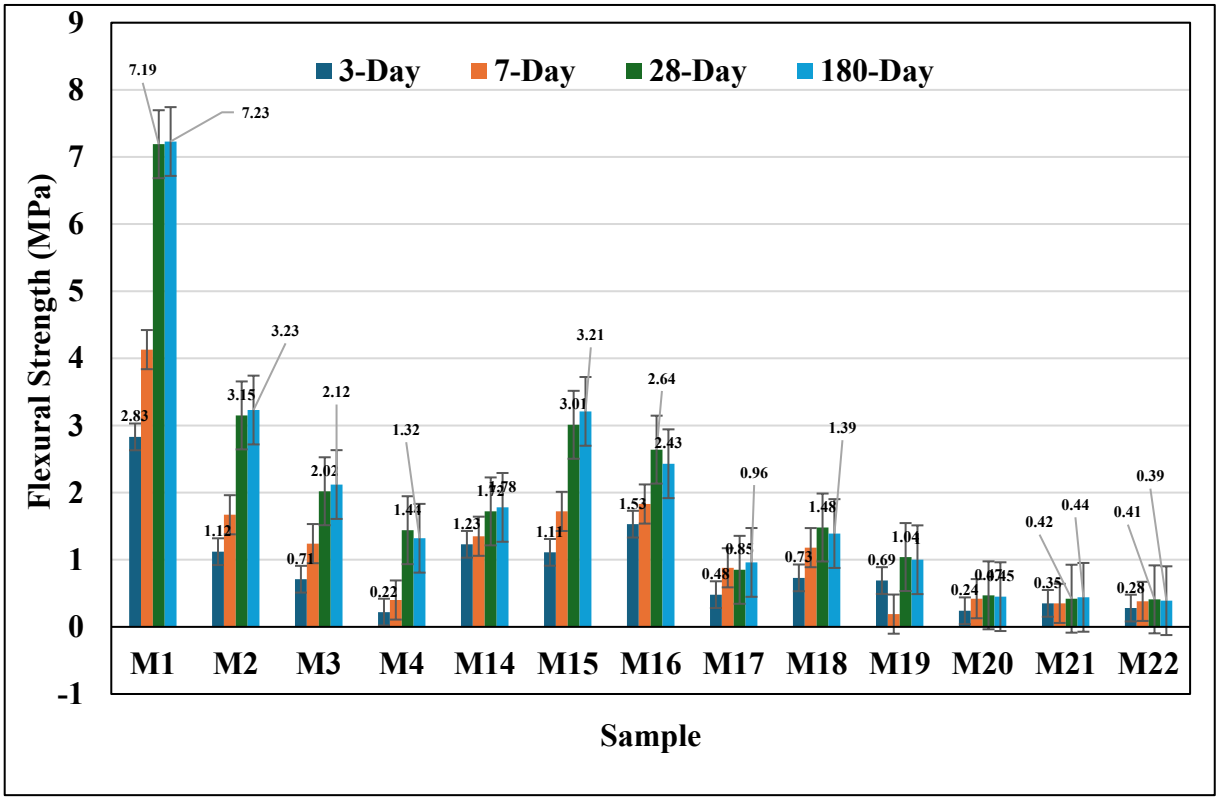


Figure 7. Flexural strength test results of geopolymer mortar specimens produced with fly ash.

Early-age tests (3 days) show that mixtures are in the initial stages of hydration and geopolymerization, exhibiting their lowest strengths. The 100% cement mixture (M1) consistently outperformed all others, reaching 7.23 MPa at 180 days, which underscores cement's critical role in matrix integrity. Conversely, increasing fly ash (FA) content significantly degraded mechanical performance due to disrupted microstructural continuity. While slag-only mixtures showed limited development, a 5% cement addition (M6, M15) emerged as the optimum threshold, yielding a 75% strength increase in FA-based mortars. Higher cement ratios (10%) failed to provide further improvements, indicating that structural

performance depends on specific slag-cement interactions rather than cement volume alone. Ultimately, high FA content and minimal cement result in inadequate mechanical properties for structural applications.

Strength gains were observed across all mixtures at 7 days, with development rates highly dependent on binder composition. For instance, M3, M6, and M15 showed significant increases in both compressive and flexural strengths, with flexural values typically ranging between 10% and 13% of the compressive strength. However, the improvement in flexural strength remained comparatively limited. This suggests that while chemical reactions progress, flexural performance is constrained by stress concentrations around fly ash (FA) inclusions and immature interfacial transition zones (ITZ) within the matrix.

Mixtures with high compressive strengths, such as M1 (100% cement) and M6 (1/4 FA, 95% slag, 5% cement), also exhibited superior flexural performance. At 28 days, M6 reached 24.2 MPa in compression and 3.15 MPa in flexure, while M1 yielded 48.51 MPa and 7.19 MPa, respectively. This trend indicates that a more compact and well-bonded geopolymer matrix not only supports higher compressive loads but also enhances tensile resistance under flexural stress.

At 28 days, experimental results showed significant mechanical gains across most mixtures. The reference M1 mixture reached 48.51 MPa in compression and 7.19 MPa in flexure (14.8% ratio), while M4 and M15 reached compressive strengths of 15.68 MPa and 23.1 MPa, with flexural-to-compressive ratios of 9.2% and 13%, respectively. A clear pattern emerges at this stage: mixtures with moderate plastic content ($\leq$25%) and blended binders exhibit superior flexural behavior relative to their compressive strength. The densified microstructure and enhanced bonding derived from synergistic pozzolanic reactions (slag/fly ash + cement) facilitate micro-crack bridging, thereby increasing resistance against flexural stresses.

By 180 days, mixtures particularly those rich in cement exhibited stabilized compressive strengths with only marginal increases in flexure, indicating limited improvements in ductility or post-crack behavior. In mixtures such as M7, M16, and M20, flexural-to-compressive strength ratios remained between 8% and 14%, with several samples showing a slight decline in flexural values despite stable compression. These results demonstrate that even at extended curing ages, mixtures with high plastic content or pure slag/fly ash (FA) binders fail to transition into ductile systems. This behavior underscores the inherently brittle nature of these geopolymer matrices, attributed to insufficient energy absorption capacity, weak FA-binder interfaces, and ineffective crack-bridging mechanisms.

3.9. Ultrasonic Pulse Velocity (UPV) Test Results of Geopolymer Mortar Specimens

Ultrasonic Pulse Velocity (UPV) was employed as a non-destructive method to evaluate the microstructural integrity and homogeneity of the geopolymer mortars (Figure 8). Generally, higher UPV values signify a denser and more continuous matrix. Results indicate that incorporating 5–10% cement into fly ash-based geopolymers significantly enhances structural integrity; for instance, the 28-day UPV increased from 1525 m/s in M14 (100% fly ash) to 1890 m/s and 2100 m/s in M15 (5% cement) and M16 (10% cement), respectively. This suggests that cement accelerates pozzolanic reactions, leading to a more compact and impermeable matrix. Conversely, increasing the fly ash (FA) ratio was found to adversely affect UPV performance, reflecting a higher void ratio and diminished connectivity (Figure 8).

Increasing the GWTR content disrupts the microstructural continuity of the geopolymer matrix, thereby obstructing the transmission of elastic waves and leading to lower UPV values. For instance, mixtures with a 1/2 GWTR ratio (M20, M21, and M22) yielded remarkably low 28-day UPV values of 680 m/s, 755 m/s, and 750 m/s, respectively. These findings

support the hypothesis that higher GWTR content results in a highly porous, inhomogeneous, and low-density internal structure, which significantly impairs wave propagation.

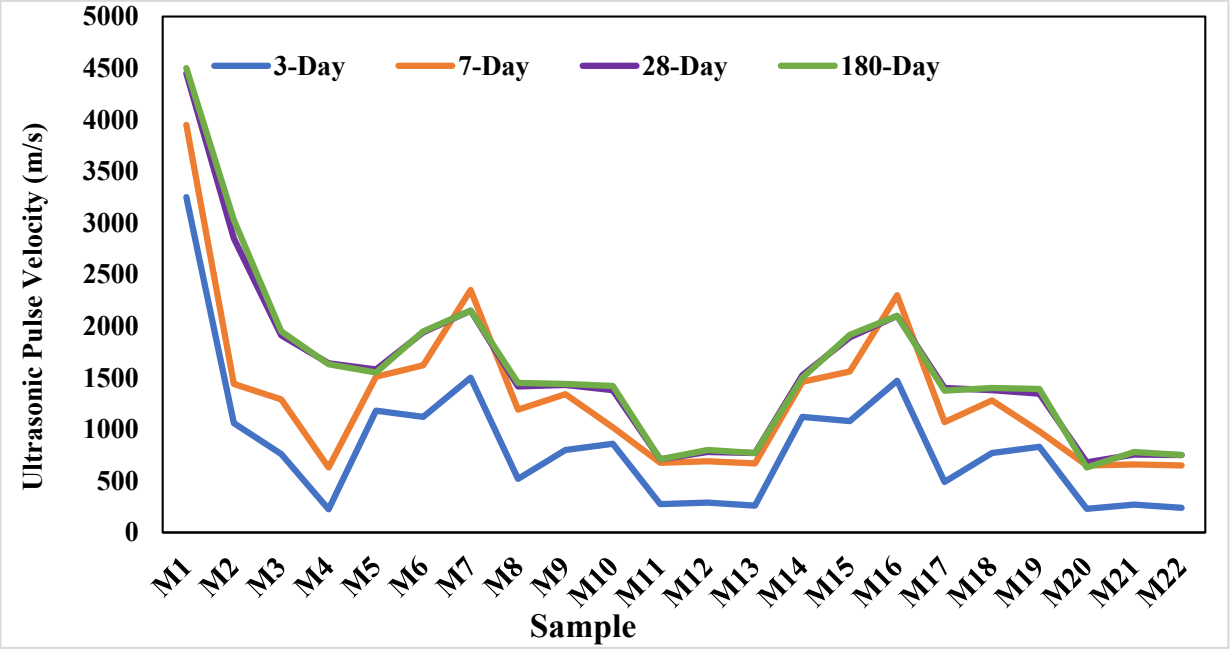


Figure 8. UPV test results of the produced geopolymer mortar specimens.

A UPV threshold of 2000 m/s is generally accepted as a critical benchmark for the quality control of structural materials via non-destructive testing. Mixtures falling below this threshold are anticipated to exhibit limited performance in structural applications. In this study, only mixtures with low GWTR content and cement additions, such as M15 and M16, successfully exceeded this limit, confirming their superior microstructural integrity compared to other geopolymer formulations.

Evaluating the mechanical performance of geopolymer-based materials is a critical step for assessing sustainability in construction. Unlike traditional compressive strength tests, which require destructive sampling, the Ultrasonic Pulse Velocity (UPV) method offers a non-destructive approach that correlates directly with material density and porosity, providing vital microstructural insights. In this study, 22 different mixtures were tested at 3, 7, 28, and 180 days. The data reveals that both GWTR content and binder composition are primary determinants of performance. Cement-based mixtures achieved the highest results (28–50 MPa in compression; 3250–4500 m/s in UPV). However, increasing the GWTR ratio particularly to ½ led to significant declines in both parameters. While slag and fly ash-based mixtures exhibited lower strengths than pure cement, the addition of 5–10% cement provided substantial mechanical enhancements.

The incorporation of GWTR significantly alters the internal stress distribution of the geopolymer matrix. While waste tire rubber does not exhibit classical swelling behavior, its presence induces a notable 'wedging effect' under mechanical loading. Due to the high contrast in elastic modulus between the rigid geopolymer binder and the soft rubber particles, the GWTR acts as a stress concentrator. Under compression, these elastic particles exert lateral pressure on the surrounding brittle matrix, functioning as internal wedges that accelerate micro-crack initiation and propagation. This phenomenon is particularly evident in mixtures with a 1/2 GWTR ratio, where the high concentration of rubber particles leads to a rapid disintegration of the structural skeleton.

3.10. SEM Analysis of Geopolymer Mortar Specimens

SEM Analysis and Microstructural Evaluation of Ferrochrome Slag-Based Geopolymers.

In this section, the microstructural characteristics of geopolymer specimens produced using ferrochrome slag one of the two primary raw materials in this study were investigated. The micrographs in Figure 9 illustrate the impact of ferrochrome slag on gel phase formation, pore architecture, and matrix homogeneity across various curing ages and mixture proportions.

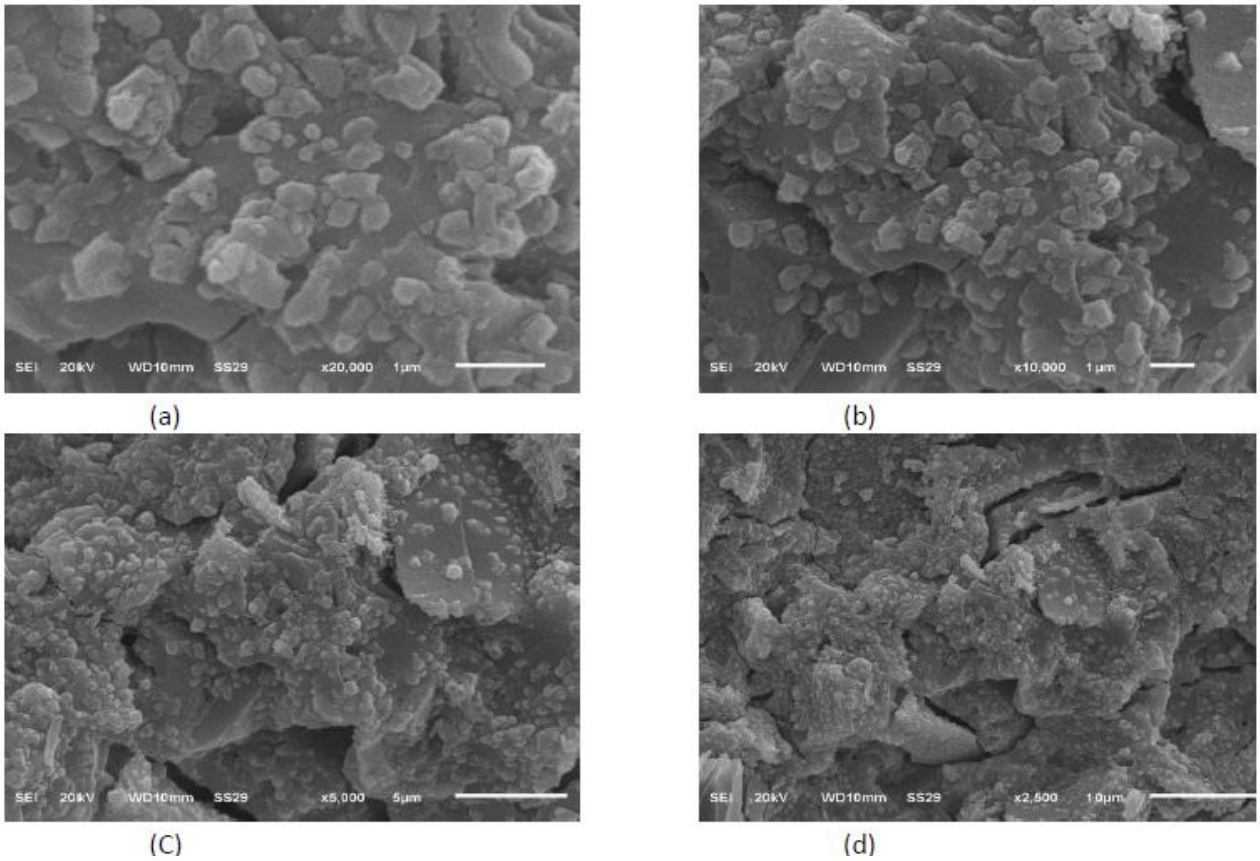


Figure 9. SEM micrographs of ferrochrome slag-based geopolymer mortars: (**a**) raw structure at 7 days of curing; (**b**) 10% cement-enhanced matrix at 28 days; (**c**) reaction cracks in high slag content matrix at 28 days; (**d**) optimized slag mixture at 28 days.

3.11. Technical Analysis of the Ferrochrome Slag-Based Micrographs

- Figure 9a (Early Age (7 Day)/Raw ferrochrome Slag Structure): This image reveals a matrix that has not yet achieved full integration. Distinctly visible angular and irregular ferrochrome slag particles suggest that the raw material has not fully dissolved, indicating the initial stages of the geopolymerization process. The lack of a continuous gel phase (C-A-S-H or N-A-S-H) provides structural evidence for the low early-age mechanical strength typically observed in these slag-based mortars.
- Figure 9b (28 Days/10% Cement-Enhanced ferrochrome Slag Matrix): With the addition of cement and the progression of curing, the ferrochrome slag-based matrix appears significantly more compact. The gel phase particles are more pronounced, effectively filling the capillary voids. Interpretation: The clusters observed suggest a "hybrid matrix" where cement hydration products interweave with the ferrochrome slag derived geopolymer gel, directly supporting the observed increases in UPV values and mechanical strength.

- Figure 9c (High ferrochrome Slag Content/Reaction Cracks): This micrograph highlights micro-cracks and irregular voids within the slag-rich matrix. Technical Commentary: These cracks likely stem from rapid chemical shrinkage or localized exothermic heat release caused by high alkali concentrations reacting with the ferrochrome slag. While a dense gel phase is present, these cracks create "weak zones" that can limit the final mechanical performance of the ferrochrome slag specimens.
- Figure 9d (Optimized Slag Mixture): This image exhibits the most homogeneous and non-porous structure among the ferrochrome slag-based specimens. The gel phase appears to cover the entire field of view. Interpretation: The continuity demonstrated here reflects a successful synergy between the ferrochrome slag and the alkali activator ratio. This low porosity maximizes both the impermeability and the long-term durability of the ferrochrome slag geopolymer.
- The lack of strong chemical bonding at the interface between the geopolymer matrix and GWTR is attributed to the hydrophobic surface of the rubber, which hinders the development of a dense ITZ. This interfacial weakness is reflected in the microstructural discontinuity and the subsequent reduction in mechanical performance.

3.12. Technical Analysis of the Fly Ash-Based Micrographs

This section evaluates the microstructural transformation of fly ash (FA), the second primary raw material of the study, from its raw state to its geopolymerized form. The impact of cement addition on the FA-matrix is analyzed through micrographs in Figure 10.

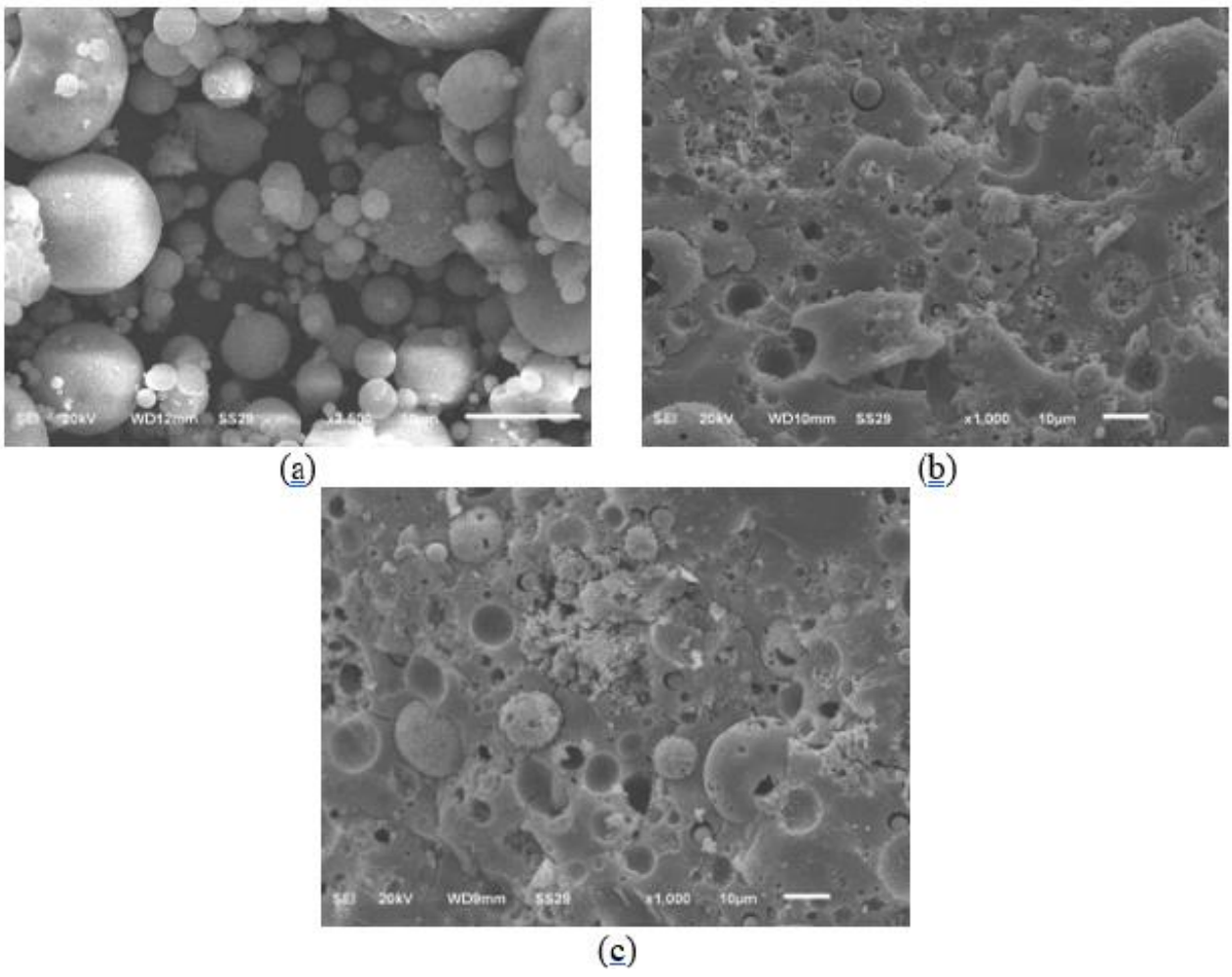


Figure 10. SEM micrographs of geopolymer mortar specimens produced with fly ash: (**a**) Raw Fly Ash; (**b**) Pure FA Geopolymer; (**c**) FA Geopolymer with 5% Cement.

- Figure 10a (Raw Fly Ash): The micrograph reveals numerous spherical particles of varying diameters, a classic characteristic of fly ash's amorphous and glassy phase. Their smooth, dense surface and wide particle size distribution are key to their high reactivity when triggered by alkali activators. This diverse sizing also allows for "particle packing," which inherently enhances the mechanical density of the final mortar.
- Figure 10b (Pure FA Geopolymer): Upon geopolymerization, the morphology shifts toward an amorphous and irregular structure. While many FA particles have dissolved into the binder, some remain partially reacted or embedded, indicating localized variations in activation. Compared to the cement-enhanced versions, this pure FA matrix appears more porous and less homogeneous, highlighting the need for a secondary binder to bridge the microstructural gaps.
- Figure 10c (FA Geopolymer with 5% Cement): The addition of 5% cement significantly refines the matrix, creating a noticeably more compact and low-porosity structure. This improvement is attributed to the formation of C-A-S-H (Calcium-Alumino-Silicate-Hydrate)-like gels alongside the geopolymer network. These hydration products act as a secondary binder phase, "filling" the micro-voids and accelerating the overall reaction rate. The result is a more unified, dense, and mechanically superior binder phase compared to the cement-free samples.

3.13. Mineralogical Characterization (XRD)

The mineralogical evolution of the geopolymer matrices was characterized through XRD analysis to elucidate the relationship between crystalline phases and mechanical performance. For slag-based geopolymers, the diffractograms exhibited a semi-crystalline nature with a prominent amorphous hump between 20° and 35° (2Θ), signifying the formation of N-A-S-H and M-A-S-H gels. Dominant crystalline peaks of Forsterite (Mg_2SiO_4) at 22.8°, 29.0°, and 43.2° (2Θ) and Spinel phases at 31.9°, 37.2°, and 44.7° were identified. These high-intensity peaks indicate a higher degree of crystallinity in the slag matrix, directly contributing to the superior compressive strength observed in these mixtures compared to fly ash counterparts (Figure 11).

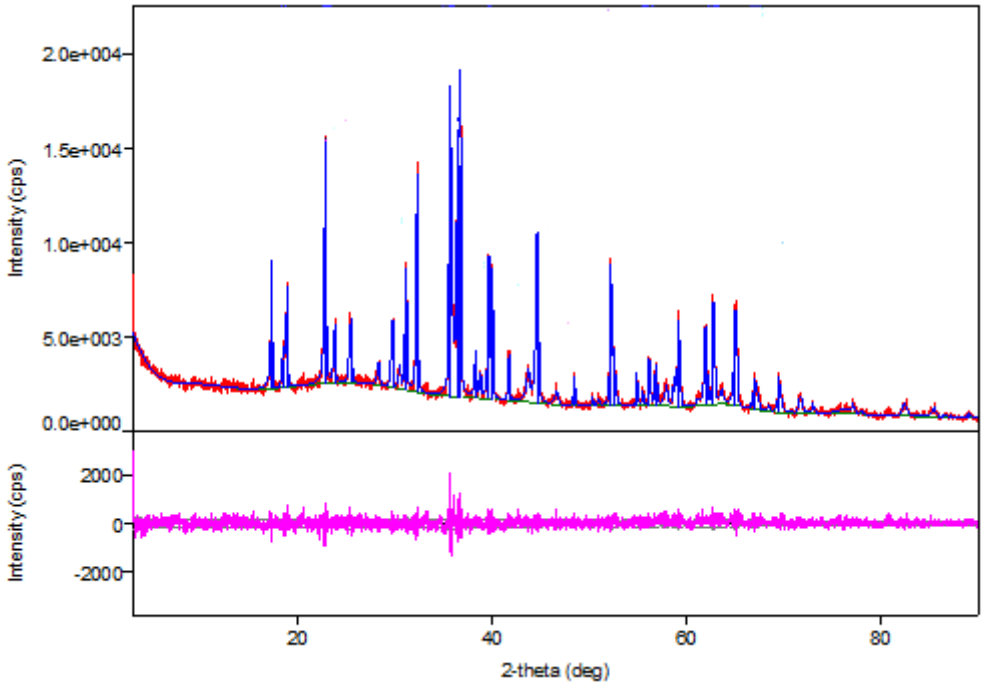


Figure 11. XRD patterns of geopolymer mortar specimens produced with ferrochrome slag.

In contrast, fly ash-based geopolymers displayed a more pronounced amorphous character with lower-intensity peaks of Cristobalite (SiO_2) and Graphite (C). The presence of Cristobalite (20.6°, 26.7°, 35.0°, 50.6°) suggests incomplete reactivity of the fly ash particles under the thermal curing regime, leading to a less dense binder matrix (Figure 12). The integration of these XRD findings with SEM observations confirms that the denser, more crystalline structure of slag-based binders provides a more robust encapsulation for GWTR particles, thereby mitigating the strength loss associated with rubber inclusion

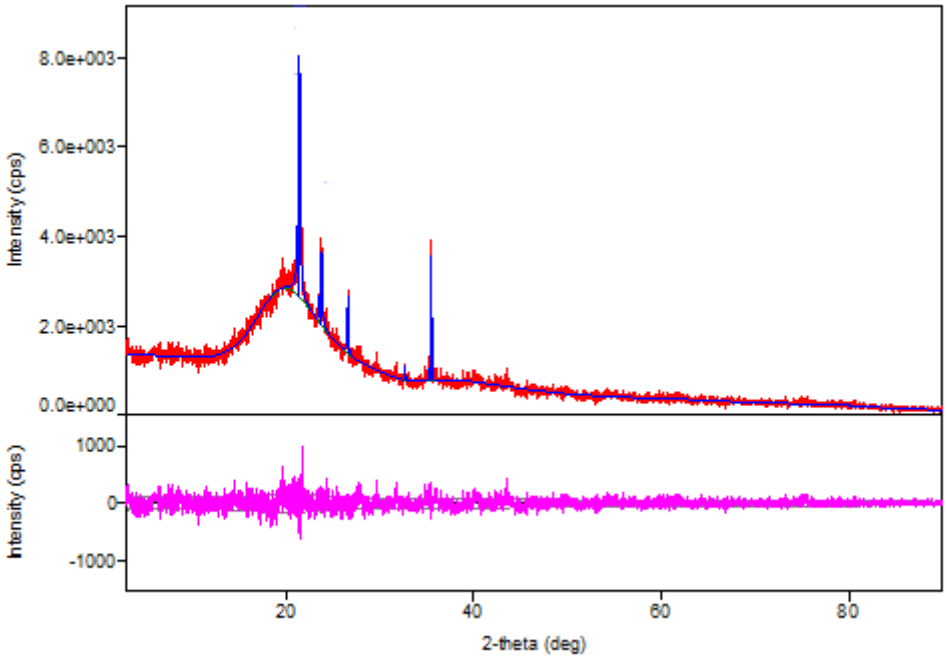


Figure 12. XRD patterns of geopolymer mortar specimens produced with fly ash.

3.14. FTIR Spectroscopic Characterization

The chemical structural evolution of the synthesized geopolymer mortars was further investigated via FTIR spectroscopy. The spectra for slag and fly ash-based specimens (Figures 13 and 14) reveal distinct vibrational modes corresponding to the degree of geopolymerization. In both systems, characteristic peaks observed between 450–500 cm^{-1} are attributed to Si-O-Si bending vibrations.

For the fly ash-based geopolymers, a broad asymmetric stretching band of Si–O–T (T = Si or Al) was identified in the 1000–1100 cm^{-1} region, indicating the formation of an amorphous aluminosilicate network. The presence of chemically and physically bound water was confirmed by the O-H stretching and H-O-H bending bands at 3400 cm^{-1} and 1650 cm^{-1}, respectively.

In contrast, the slag-based specimens exhibited a shift in the Si–O–T band toward lower wavenumbers (~950–1000 cm^{-1} with a sharper profile. This shift, driven by the high CaO content of the ferrochrome slag, signifies a different reaction pathway leading to the formation of C-A-S-H like gels. Furthermore, the bands observed at 1400–1450 cm^{-1} correspond to CO_3^{2-} vibrations, suggesting minor carbonation through the reaction of calcium with atmospheric CO_2. The distinct Al–O vibrations near 870 cm^{-1} in slag samples further support the development of a more unified and dense binder phase compared to fly ash systems.

The use of ferrochrome slag and GWTR as substitutes for Portland cement offers significant economic and practical advantages. By reducing material costs and minimizing environmental taxes associated with landfilling industrial waste, these geopolymer mortars provide a cost-effective alternative. Practically, their high early-age strength makes them

ideal for precast applications like pavement blocks and acoustic barriers, supporting a sustainable circular economy in the construction sector.

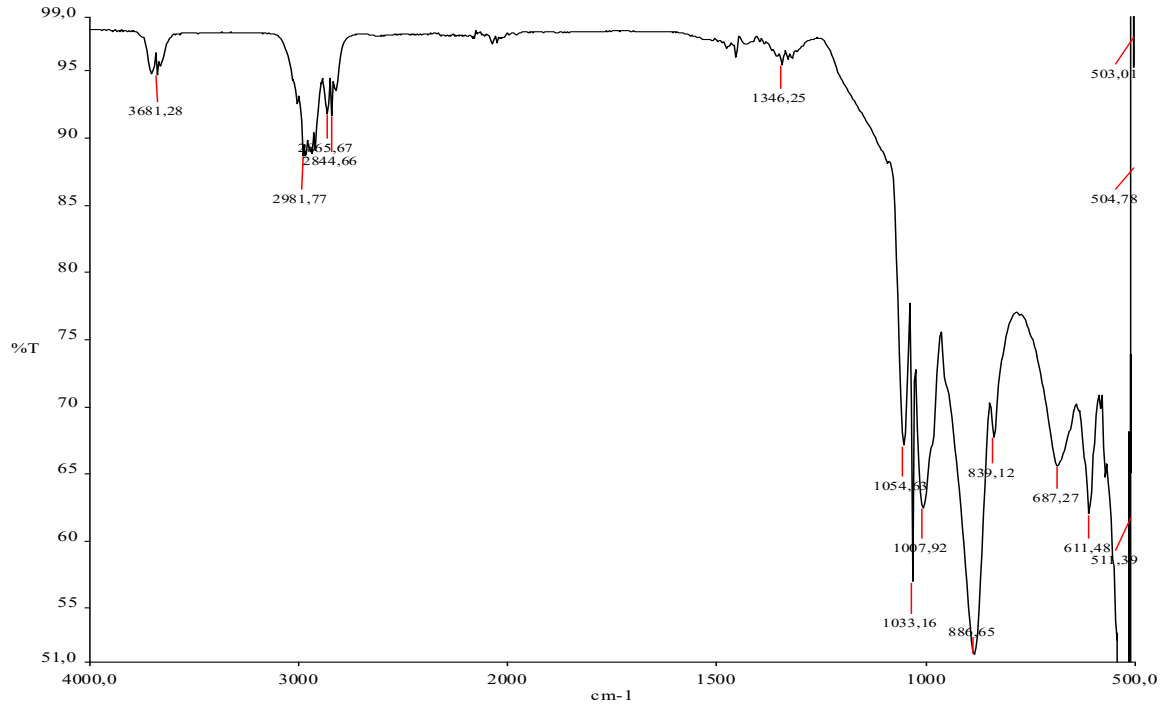


Figure 13. FTIR spectra of geopolymer mortar specimens produced with ferrochrome slag.

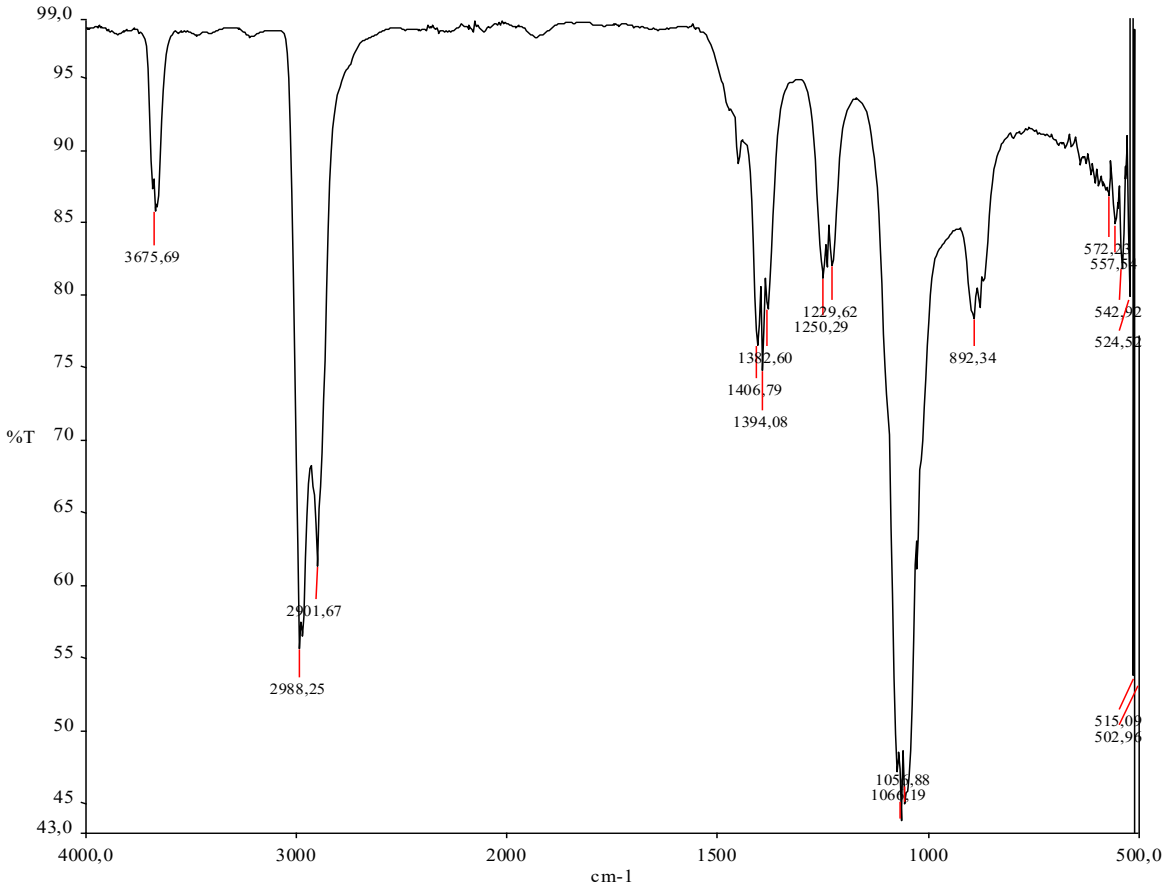


Figure 14. FTIR spectra of geopolymer mortar specimens produced with fly ash.

4. Conclusions

In this study, the short- and long-term mechanical and physical performances of mixtures prepared by incorporating specific ratios of GWTR waste into cement paste and utilizing alternative binders (slag and fly ash) were evaluated. The experimental findings elucidate the impact of alternative binder materials on performance aimed at enhancing environmental sustainability.

The following conclusions were drawn from the analysis of mixture proportions, flexural and compressive strength tests, ultrasonic pulse velocity (UPV) measurements, and SEM analyses:

- Impact of GWTR: Since GWTR lacks binding properties particularly in cement-based systems it led to a reduction in both compressive and flexural strengths. Furthermore, it caused significant declines in UPV values due to the microstructural discontinuity it creates within the matrix.
- Structural Integrity: The cement-based mixture containing 1/2 GWTR by volume (M4) yielded a 28-day compressive strength of 15.68 MPa, whereas the 100% cement reference mixture (M1) reached 48.51 MPa. This indicates that while GWTR functions similarly to aggregate, it has a weakening effect on structural integrity.
- Synergistic Effects of Binders: The use of pozzolanic materials like slag and fly ash in the geopolymer matrix can partially compensate for GWTR induced strength losses. Specifically, incorporating 5–10% cement into these matrices enhances reactivity, leading to significant improvements in both early and late-age strengths.
- Optimal Mixtures: Results from M6, M7, M15, and M16 demonstrate that these formulations stand out as viable alternatives for both technical performance and the mitigation of environmental impacts. Mixtures with an optimized 1/4 GWTR ratio provided the most balanced strength results.
- Long-term Development: Performance data from 180-day tests confirmed that geopolymer mixtures with appropriate binder additives gain strength over time. The late-reaction tendency of fly ash-based geopolymers was verified; despite lower early-age strengths, their mechanical properties continued to improve through prolonged pozzolanic activity.
- UPV and Microstructure: A direct correlation was observed between UPV values and compressive strength. Lower UPV values were associated with internal voids, weak bonding, or micro-cracks resulting from incomplete reactions or curing conditions. Thus, UPV provides vital data not only on strength but also on microstructural integrity.
- Material Characterization: Slag-based geopolymers exhibit a denser, calcium- and aluminum-rich structure, whereas fly ash-based counterparts are more amorphous and silica-rich with higher water retention.

Final Remark: While GWTR does not exhibit independent binding properties and negatively affects mechanical performance when used alone, its integration into geopolymer matrices alongside industrial wastes (GGBS/FA) and minor cement substitution enables the production of eco-friendly alternative materials with acceptable structural properties.

Based on the experimental results, the optimal substitution level for Granulated Waste Tire Rubber (GWTR) was identified as 25% by volume of the total aggregate (a 1/4 ratio). At this specific dosage, the geopolymer mortars (particularly mixtures M6, M7, M15, and M16) achieved the most favorable balance between mechanical performance and environmental sustainability. While higher rubber contents led to a more pronounced decline in compressive strength and UPV values, the 1/4 replacement ratio allowed for the successful integration of waste tires into the geopolymer matrix without compromising structural integrity, offering a viable path for eco-friendly construction materials.

https://doi.org/10.3390/buildings16091751

In summary, FTIR spectroscopic analysis clearly distinguishes the structural characteristics of the two binder systems. Slag-based geopolymers exhibit a significantly denser, calcium- and aluminum-rich matrix, whereas fly ash-based systems lean toward a more amorphous, silica-rich framework with higher water retention capacity. These spectral findings confirm that while both industrial by-products are highly viable for sustainable geopolymer production, they offer distinct structural properties and performance pathways. Ultimately, the FTIR data provides a molecular-level validation of these differences, allowing for a more strategic selection of binder types based on specific engineering requirements.

5. Limitations and Future Recommendations

Although this study provides significant insights into the integration of GWTR into slag and fly ash-based geopolymers, certain limitations should be acknowledged. Firstly, the fresh-state properties were primarily characterized by setting time, and a more detailed rheological investigation could provide further clarity on the workability of these complex mixtures. Secondly, the long-term durability performance, including freeze–thaw resistance and sulfate attack, remains to be explored to ensure outdoor structural reliability.

For future research, it is recommended to investigate chemical or thermal surface treatments of GWTR particles to enhance the interfacial bonding with the geopolymer matrix. Additionally, performing a comprehensive Life Cycle Assessment (LCA) and a detailed cost–benefit analysis would be beneficial to validate the large-scale industrial feasibility and environmental impact of these sustainable mortars in the construction sector.

Author Contributions: Conceptualization, M.M.; methodology, M.M.; software, E.B. and M.M.; validation, M.M. and E.B.; formal analysis, E.B. and M.M.; investigation, E.B.; resources, M.M.; data curation, E.B.; writing, original draft preparation, E.B. and M.M.; writing—review and editing, M.M.; visualization, E.B.; supervision, M.M.; project administration, M.M. All authors have read and agreed to the published version of the manuscript.

Funding: This research received no external funding.

Data Availability Statement: Data are contained within the article.

Acknowledgments: Portions of this study were refined using AI-assisted technologies for language editing and academic translation to enhance the clarity of the technical analysis. The authors reviewed and approved all generated content before submission.

Conflicts of Interest: The authors declare no conflict of interest.

References

1. Luhar, S.; Cheng, T.-W.; Nicolaides, D.; Luhar, I.; Panias, D.; Sakkas, K. Valorisation of glass wastes for the development of geopolymer composites–Durability, thermal and microstructural properties: A review. *Constr. Build. Mater.* **2019**, *222*, 673–687. [CrossRef]
2. Luhar, I.; Luhar, S. Rubberized geopolymer composites: Value-added applications. *J. Compos. Sci.* **2021**, *5*, 312. [CrossRef]
3. Davidovits, J. *Geopolymer Chemistry and Applications*; Geopolymer Institute: Saint-Quentin, France, 2008.
4. Bondar, D. Alkali Activation of Iranian Natural Pozzolans for Producing Geopolymer Cement and Concrete. Ph.D. Thesis, University of Sheffield, Sheffield, UK, 2009.
5. Aly, A.M.; El-Feky, M.; Kohail, M.; Nasr, E.-S.A. Performance of geopolymer concrete containing recycled rubber. *Constr. Build. Mater.* **2019**, *207*, 136–144. [CrossRef]
6. Torgal, F.P.; Labrincha, J.A.; Leonelli, C.; Palomo, A.; Chindaprasirt, P. *Handbook of Alkali-Activated Cements, Mortars and Concretes*; Woodhead Publishing: Cambridge, UK, 2015.
7. Chen, R.; Li, Q.; Zhang, Y.; Xu, X.; Zhang, D. Pyrolysis kinetics and mechanism of typical industrial non-tyre rubber wastes by peak-differentiating analysis and multi kinetics methods. *Fuel* **2019**, *235*, 1224–1237. [CrossRef]
8. Flower, D.J.; Sanjayan, J.G. Green house gas emissions due to concrete manufacture. *Int. J. Life Cycle Assess.* **2007**, *12*, 282–288. [CrossRef]

9. Arunkumar, K.; Muthukannan, M.; Kumar, A.S.; Ganesh, A.C. Mitigation of waste rubber tire and waste wood ash by the production of rubberized low calcium waste wood ash based geopolymer concrete and influence of waste rubber fibre in setting properties and mechanical behavior. *Environ. Res.* **2021**, *194*, 110661. [CrossRef]
10. Kajaste, R.; Hurme, M. Cement industry greenhouse gas emissions–management options and abatement cost. *J. Clean. Prod.* **2016**, *112*, 4041–4052. [CrossRef]
11. Siddique, R.; Naik, T.R. Properties of concrete containing scrap-tire rubber–an overview. *Waste Manag.* **2004**, *24*, 563–569. [CrossRef]
12. Medine, M.; Trouzine, H.; Barroso De Aguiar, J.; Djadouni, H. Life cycle assessment of concrete incorporating scrap tire rubber: Comparative study. *Rev. Nat. Technol.* **2020**, *12*, 1–11.
13. Saad, A.G.; Sakr, M.A.; Khalifa, T.M.; Darwish, E.A. Structural performance of concrete reinforced with crumb rubber: A review of current research. *Iran. J. Sci. Technol. Trans. Civ. Eng.* **2025**, *49*, 3211–3254. [CrossRef]
14. Ralli, Z.G.; Pantazopoulou, S.J. Pantazopoulou, State of the art on geopolymer concrete. *Int. J. Struct. Integr.* **2021**, *12*, 511–533. [CrossRef]
15. Pham, T.M.; Liu, J.; Tran, P.; Pang, V.-L.; Shi, F.; Chen, W.; Hao, H.; Tran, T.M. Dynamic compressive properties of lightweight rubberized geopolymer concrete. *Constr. Build. Mater.* **2020**, *265*, 120753. [CrossRef]
16. Luhar, S.; Chaudhary, S.; Luhar, I. Development of rubberized geopolymer concrete: Strength and durability studies. *Constr. Build. Mater.* **2019**, *204*, 740–753. [CrossRef]
17. Kuang, F.; Long, Z.; Kuang, D.; Guo, R.; Sun, J. Experimental study on preparation and properties of low content rubberized geopolymer mortar. *Constr. Build. Mater.* **2022**, *352*, 128980. [CrossRef]
18. Lazorenko, G.; Kasprzhitskii, A.; Mischinenko, V. Rubberized geopolymer composites: Effect of filler surface treatment. *J. Environ. Chem. Eng.* **2021**, *9*, 105601. [CrossRef]
19. Zhang, B.; Feng, Y.; Xie, J.; Lai, D.; Yu, T.; Huang, D. Rubberized geopolymer concrete: Dependence of mechanical properties and freeze-thaw resistance on replacement ratio of crumb rubber. *Constr. Build. Mater.* **2021**, *310*, 125248. [CrossRef]
20. Wongsa, A.; Sata, V.; Nematollahi, B.; Sanjayan, J.; Chindaprasirt, P. Mechanical and thermal properties of lightweight geopolymer mortar incorporating crumb rubber. *J. Clean. Prod.* **2018**, *195*, 1069–1080. [CrossRef]
21. Ferreira, R.d.R.; Gratão, L.; Motta, L.d.C. Evaluation and optimization of the replacement of fine aggregate by waste tire rubber in geopolymer mortar with metakaolin. *Mech. Compos. Mater.* **2024**, *59*, 1223–1238. [CrossRef]
22. Mermerdaş, K.; İpek, S.; Işıker, Y.; Rasool, H. Effect of waste tire aggregate on thermal and strength characteristics of fly ash–based geopolymer composites produced at various binder contents. *J. Mater. Civ. Eng.* **2023**, *35*, 04023355. [CrossRef]
23. Mabrouk, A.; Raza, A.; Elhadi, K.M.; Ahmed, B.; Kubica, J.; Chen, W. Effect of curing temperature, silica fume, and waste tire rubber aggregate on material characterization of lightweight geopolymer composite. *Constr. Build. Mater.* **2024**, *453*, 139063. [CrossRef]
24. Yadollahi, M.M.; Varolgüneş, S.; İşsever, F. Na_2O, silika modülü, su/bağlayıcı oranı ve yaşlanmanın cüruf tabanlı geopolimerlerin basınç mukavemetinde olan etkileri. *Türk Doğa Fen Derg.* **2017**, *6*, 26–31.
25. Mohabbı, M. Nano silica and micro silica effect on mechanical attributes of ferrochrome slag based geopolymer. *Duzce Univ. J. Sci. Technol.* **2020**, *8*, 347–362. [CrossRef]
26. Mohabbı, M.; Kolak, M.N. Investigation of Waste Mineral Wool in Geopolymer Production. *Türk Doğa Fen Derg.* **2024**, *13*, 192–198. [CrossRef]
27. Parveen; Singhal, D.; Junaid, M.T.; Jindal, B.B.; Mehta, A. Mechanical and microstructural properties of fly ash based geopolymer concrete incorporating alccofine at ambient curing. *Constr. Build. Mater.* **2018**, *180*, 298–307. [CrossRef]
28. Matsimbe, J.; Dinka, M.; Olukanni, D.; Musonda, I. Geopolymer: A systematic review of methodologies. *Materials* **2022**, *15*, 6852. [CrossRef]
29. Tchakouté, H.K.; Rüscher, C.H. Mechanical and microstructural properties of metakaolin-based geopolymer cements from sodium waterglass and phosphoric acid solution as hardeners: A comparative study. *Appl. Clay Sci.* **2017**, *140*, 81–87. [CrossRef]
30. Yadollahi, M.M.; Demirboğa, R.; Polat, R. Effect of heat treatment temperature on ground pumice activation in geopolymer composites. *Sci. Eng. Compos. Mater.* **2014**, *21*, 377–382. [CrossRef]
31. Yadollahi, M.M.; Benli, A.; Demirboğa, R. The effects of silica modulus and aging on compressive strength of pumice-based geopolymer composites. *Constr. Build. Mater.* **2015**, *94*, 767–774. [CrossRef]
32. Yadollahi, M.M.; Benli, A. Stress-strain behavior of geopolymer under uniaxial compression. *Comput. Concr.* **2017**, *20*, 381–389.
33. Bayrak, B.; Ipek, S.; Alcan, H.G.; Kaplan, G.; Aydın, A.C.; Güneyisi, E. Engineering and microstructural properties of environmentally friendly alkali-activated composites containing clinker aggregate: Heat-curing regime and elevated-temperature effect. *Arch. Civ. Mech. Eng.* **2024**, *24*, 200. [CrossRef]
34. Yadollahi, M.M.; Dener, M. Investigation of elevated temperature on compressive strength and microstructure of alkali activated slag based cements. *Eur. J. Environ. Civ. Eng.* **2021**, *25*, 924–938. [CrossRef]

35. *ASTM C348-21*; Standard Test Method for Flexural Strength of Hydraulic-Cement Mortars. American Society of Testing Materials: West Conshohocken, PA, USA, 2008.
36. *ASTM C109/C109M-20*; Standard Test Method for Compressive Strength of Hydraulic Cement Mortars (Using 2-in. or [50-mm] Cube Specimens). American Society of Testing Materials: West Conshohocken, PA, USA, 2013.

Disclaimer/Publisher's Note: The statements, opinions and data contained in all publications are solely those of the individual author(s) and contributor(s) and not of MDPI and/or the editor(s). MDPI and/or the editor(s) disclaim responsibility for any injury to people or property resulting from any ideas, methods, instructions or products referred to in the content.